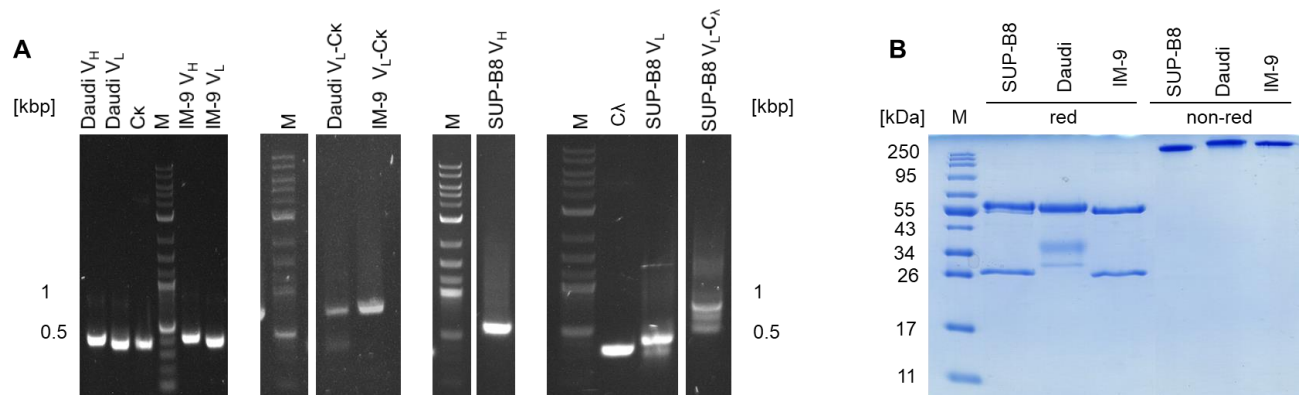


Supplementary Material

1 Supplementary Figures



SUPPLEMENTARY FIGURE S1 | Generation of B-cell lymphoma-derived soluble BCR protein. BCR-coding genes were amplified separately using different primers binding in the FR1 and C_L/C_{H1} regions. For heavy chains, V_H domains of matuzumab were exchanged for the identified BCR V_H domains. For light chains, V_L of Daudi and IM-9 were fused *via* PCR to C_{Kappa} domains, V_L of SUP-B8 to C_{Lambda}, respectively (A). Reducing SDS-PAGE of BCRs after expression in HEK 293F cells (B). Using matuzumab as a scaffold, the respective V_H and V_L domains were exchanged for the identified BCR-derived variable domains. Purification was performed using Protein A spin columns. Molecular weight of heavy chains is approximately 55 kDa, of light chains ~26 kDa, respectively.

SUP-B8 Heavy Chain

	CDR-H1
published	QIQLVQSGGEVKKPGASVRVSKASGYTFHSGYITWVRQAPGQGLEWMG
VH1	...LVQSGGEVKKPGASVKVSKASGYTFHSGYITWVRQAPGQGLEWMG
VH2VSKASGYTFHSGYITWVRQAPGQGLEWMG
VH5	..QLVQSGGEVKKPGASVKVSKASGYTFHSGYITWVRQAPGQGLEWMG
	CDR-H2
published	WISGYNGNTNYAQKLQDRVTMTTDTSTNTVYMEVRSRLRSDDTAVYYCAR
VH1	WINGYNGYTNYAQKLQDRVTMTTNTSTNTVYMEVRSRLRSDDTAVYYCAR
VH2	WINGYNGYTNYAQKLQDRVTMTTNTSTNTVYMEVRSRLRSDDTAVYYCAR
VH5	WINGYNGYTNYAQKLQDRVXMTTNTSTNTVYMEVRSRLRSDDTAVYYCAR
	CDR-H3
published	DDCSGDNCYMSAYWGQGLVTVSS
VH1	DDCSGDNCYMSAYWGQGTVVTVSS
VH2	DDCSGDNCYMSAYWGQGTVVTVSS
VH5

SUP-B8 Light Chain

	CDR-L1	CDR-L2
published	QSVLTQPPSASGTPGQRVTISC	SGSSSKIASNYVYWYQQVPGTAPKLLIYRDNQRPSGV
IgL_36-47	QSVLTQPPSASGTPGQRVTISC	SGSSSNIASNYVYWYQQLPGMAPKLLIYRDNQRPSGV
IgL_51	QSVLTQPPSASGTPGQRVTISC	SGSSSNIASNYVYWYQQLPGMAPKLLIYRDNQRPSGV
	CDR-L3	
published	PDRFSGSRSGTSASLAI	SGLRSDDEADYYCATWDDSLSGWVFGGGTKLTVL
IgL_36-47	PDRFSGSRSGTSASLAI	SGLRSDDEADYYCATWDDSLSGWVFGGGTKLTVL
IgL_51	PDRFSGSRSGTSASLAI	SGLRSDDEADYYCATWDDSLSGWVFGGGTKLTVL

IM-9 Heavy Chain

	CDR-H1
published	LEVQLVESGGGLLQPGRALRLSCAASGFRFD
VH3_revVESGGGLLQPGRALRLSCAASGFRFD
VH1_revVQSGGGLLQPGRALRLSCAASGFRFD
VH1_fwd_upRFDDYAMHWVRQTPGKGLEWVA
3_fwd_upRFDDYAMHWVRQTPGKGLEWVA
5_fwd_upFDDYAMHWVRQTPGKGLEWVA
	CDR-H2
published	GISWNSDTIDYADSVKGRFTISRDNAKNSLYLQMN
VH3_rev	GISWNSDTIDYADSVKGRFTISRDNAKNSLYLQMN
VH1_rev	GISWNSDTIDYADSVKGRFTISRDNAKNSLYLQMN
VH1_fwd_up	GISWNSDTIDYADSVKGRFTISRDNAKNSLYLQMN
3_fwd_up	GISWNSDTIDYADSVKGRFTISRDNAKNSLYLQMN
5_fwd_up	GISWNSDTIDYADSVKGRFTISRDNAKNSLYLQMN
	CDR-H3
published	GGVTDIDPFDIWGQGMVIVSS
VH3_rev	RGVTDIDPF.....
VH1_rev	RGVTDIDPF.....
VH1_fwd_up	RGVTDIDPFDIWGQGMVIVSS
3_fwd_up	RGVTDIDPFDIWGQGMVIVSS
5_fwd_up	RGVTDIDPFDIWGQGMVIVSS

IM-9 Light Chain

	CDR-L1	CDR-L2
published	ELQMTQSPSTLSASVGDRVTITCRASQSI	PWLPWYQQKPGKAPKLLIYKASSLES
Vk2_loTQSPSTLSASVGDRVTITCRASQSI	SAWLAWYQQKPGKAPKLLIYKASSLES
Vk1_upSISAWLAWYQQKPGKAPKLLIY	KASSLES
	CDR-L3	
published	RFSGSGSGTEFTLTITSLQPDDFATYFC	QHYNRPWTFGQGTKVEIKR
Vk2_lo	RFSGSGSGTEFTLTITSLQPDDFATYFC	QHYNRPWT.....
Vk1_up	RFSGSGSGTEFTLTITSLQPDDFATYFC	QHYNRPWTFGQGTKVEIKR

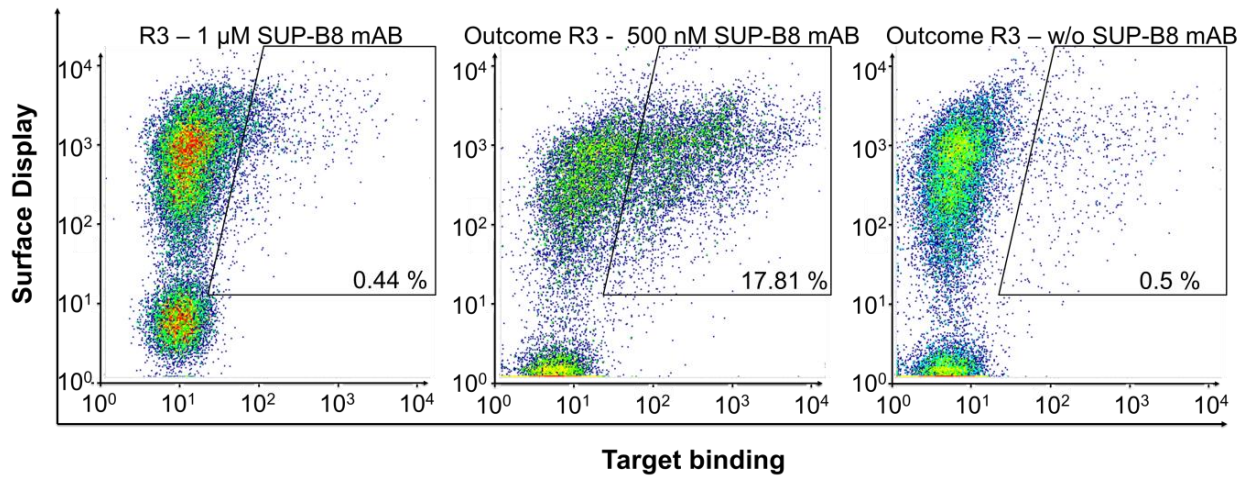
Daudi Heavy Chain

	CDR-H1
published	LEVQLVESGGN N LVQPGGSLRLSCE V SGF S ITSY G IHWVRQAPGKGLVWVS
VH3	LEVQLVESGGDLVQPGGSLRLSCEASGFTITSYGMHWVRQAPGKGLVWVS
VH5_fwd	...QLVESGGDLVQPGGSLRLSCEASGFTITSYGMHWVRQAPGKGLVWVS
VH5_rev
	CDR-H2
published	E TDNDGRDATYADSVKGRFTSLPDRANNTLYLQMN S LRVDDTAVYYCVRG
VH3	EIDNDGRDATYADSVKGRFTSLPDRANNTLYLQMN S LRVDDTAVYYCVRG
VH5_fwd	EIDNDGRDATYADSVKGRFTSLPDRANNTLYLQMN S LRVDDTAVYYCVRG
VH5_revDATYADSVKGRFTSLPDRANNTLYLQMN S LRVDDTAVYYCVRG
	CDR-H3
published	NGQKCFDYWGQTLVTVSS
VH3	NGQKCFDYWGQTLVTVSS
VH5_fwd	NGQKCFDYW.....
VH5_rev	NGQKCFDYWGQTLVTVSS

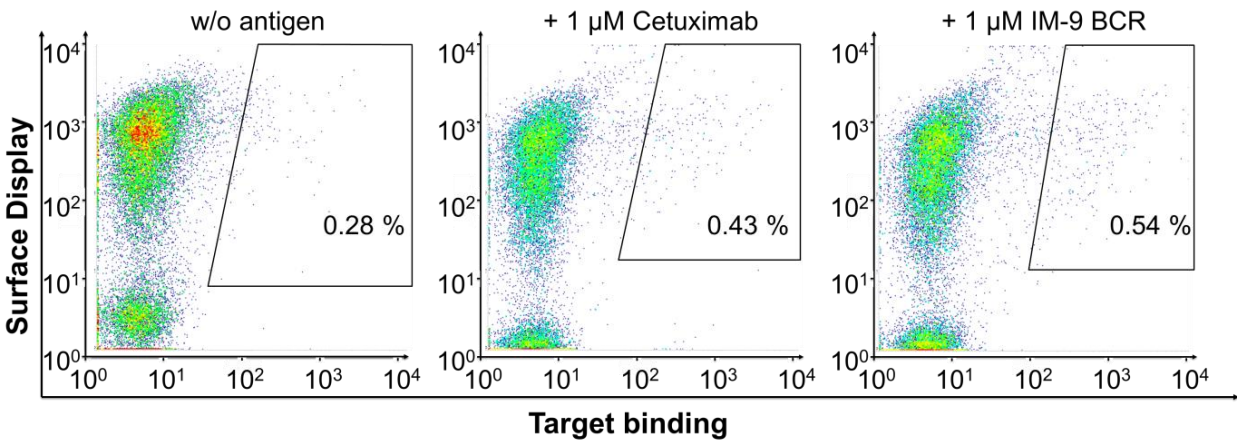
Daudi Light Chain

	CDR-L1	CDR-L2
published	ELQMTQSPSSLSA S VGDRVTITCRAGHNI T NFLSWYQQKPGKAP T LLIYAVSNLQ D GV	
Vk1_upTQSPSSLSACVGDRVTITCRAGHNI T NFLSWYQQKPGKAP T LLIYAVSNLQ R GV	
Vk1_loTQSPSSLSACVGDRVTITCRAGHNI T NFLSWYQQKPGKAP T LLIYAVSNLQ R GV	
Vk2_upVTITCRAGHNI T NFLSWYQQKPGKAP T LLIYAVSNLQ R GV	
	CDR-L3	
published	PSRFSGSGSGAEFTLTIS S LQPEDFATYYC Q QNYN F S F T F GGG T KVDN K R	
Vk1_up	PSRFSGSGSGAEFTLTIS S LQPEDFATYYC Q QNYN F S F T F GGG T KVDN K R	
Vk1_lo	PSRFSGSGSGAEFTLTIS S LQPEDFATYYC Q QNYN F S F T F GGG .	
Vk2_up	PSRFSGSGSGAEFTLTIS S LQPEDFATYYC Q QNYN F S F T F GGG T KVDN K R	

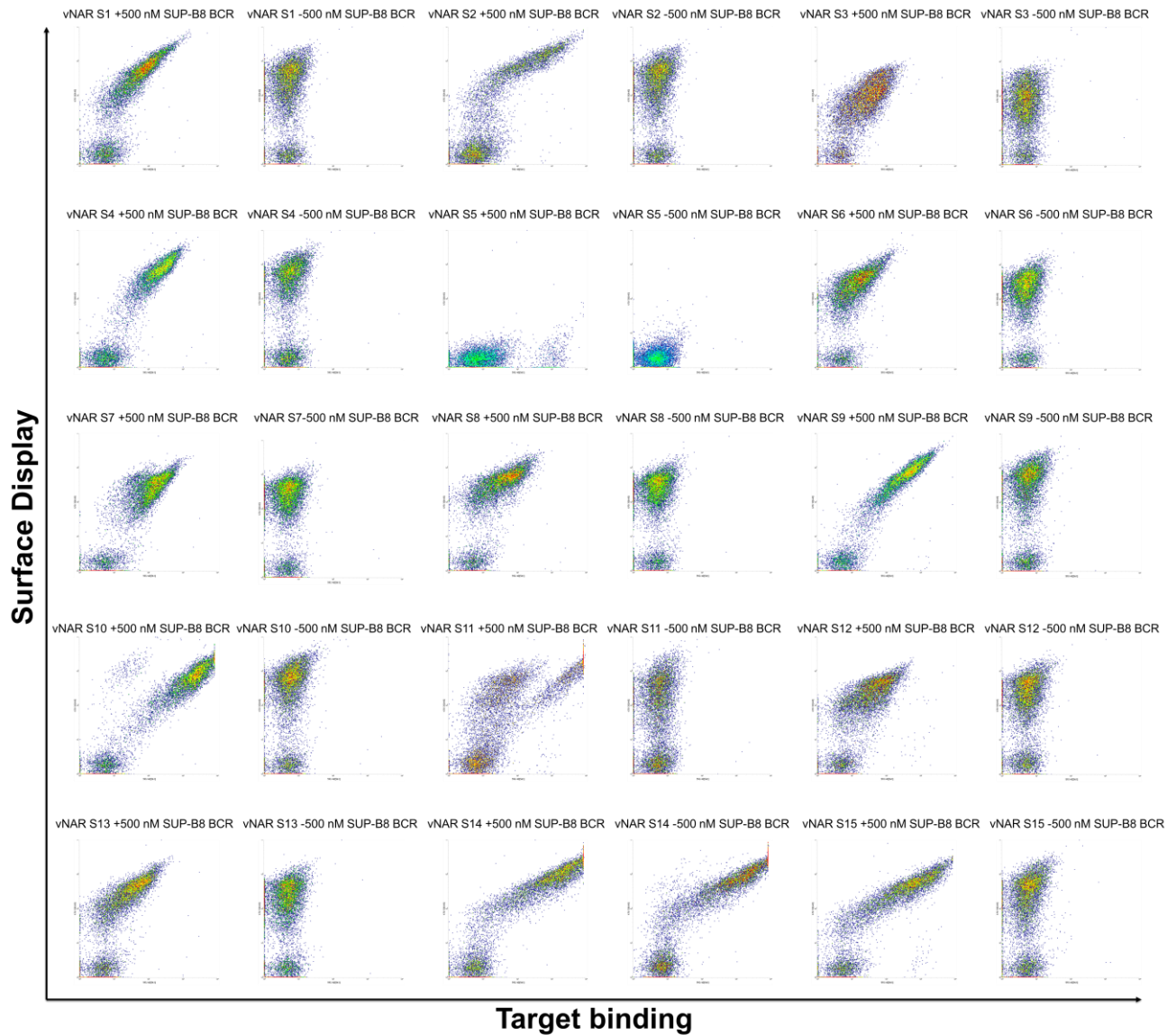
SUPPLEMENTARY FIGURE S2 | Sequence overview over 3 BCRs from 3 different lymphoma cell lines Daudi, IM-9 and SUP-B8. After RNA extraction and cDNA synthesis BCR-coding genes were amplified separately using different primers binding in the FR1 and CL/CH1 regions. The resulting sequences were aligned to the published sequences, variations are depicted in red. The CDR boundaries are indicated above the sequence alignment.



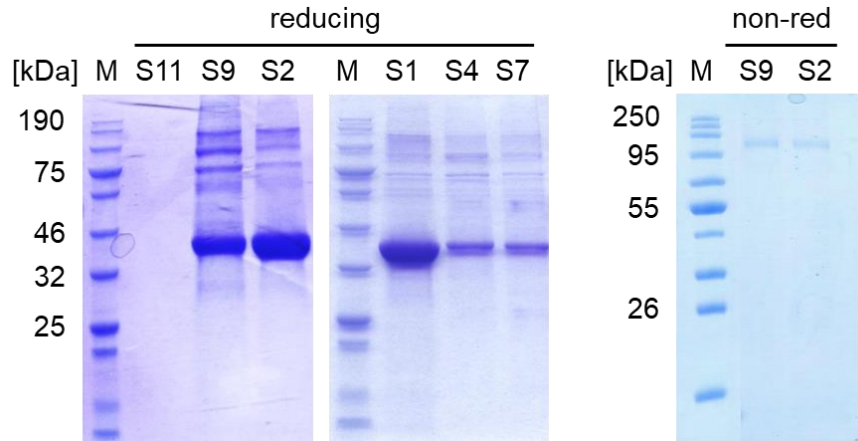
SUPPLEMENTARY FIGURE S3 | Shark-derived vNAR library screening against the BCR of cell line SUP-B8. In addition to the third screening round stained with anti-Human Fc-PE, the third round of screening was performed in parallel with antigen stained with anti-Human Lambda-PE. Sorting gates, percentages of cells in the respective gate and target concentrations are shown. One day after induction, yeast cells were labeled for parallel detection of antigen-binding and surface presentation. After screening cells in the sorting gate were isolated, grown and induced for the next round of selection.



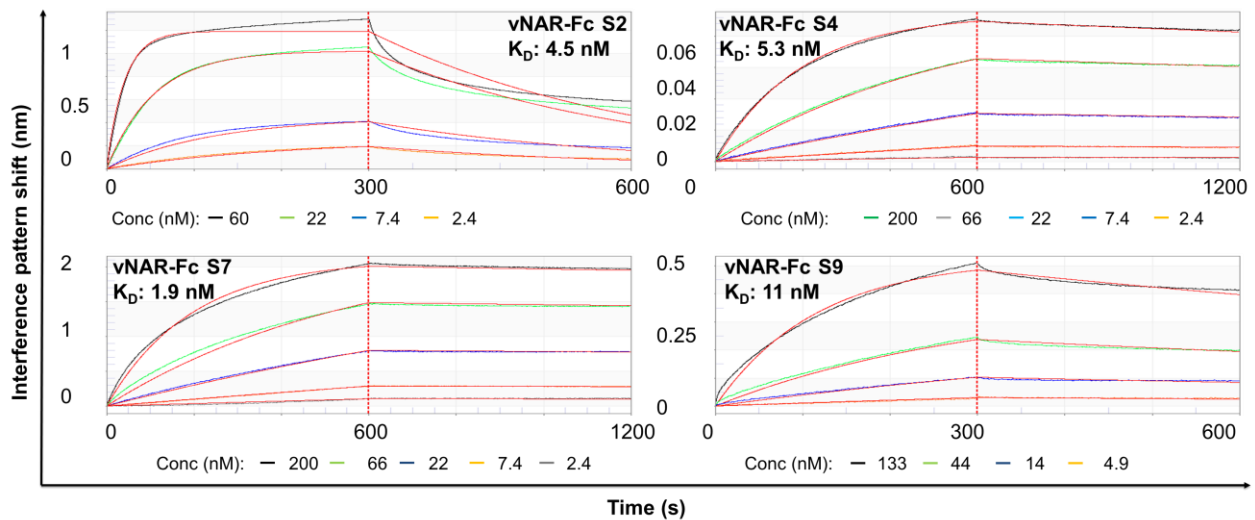
SUPPLEMENTARY FIGURE S4 | Specificity of vNAR-presenting yeast population after two rounds of sorting for SUP-B8-BCR binding variants as determined via binding assays on the yeast surface. A negative control in absence of antigen was performed whilst off-target binding was validated against the unrelated antibody cetuximab and the BCR of cell line IM-9. Surface presentation was detected by utilizing anti-myc biotin and SAPC, target binding was analyzed by using anti-human-FC PE conjugate. The percentage of cells localized in gate is depicted on each plot.



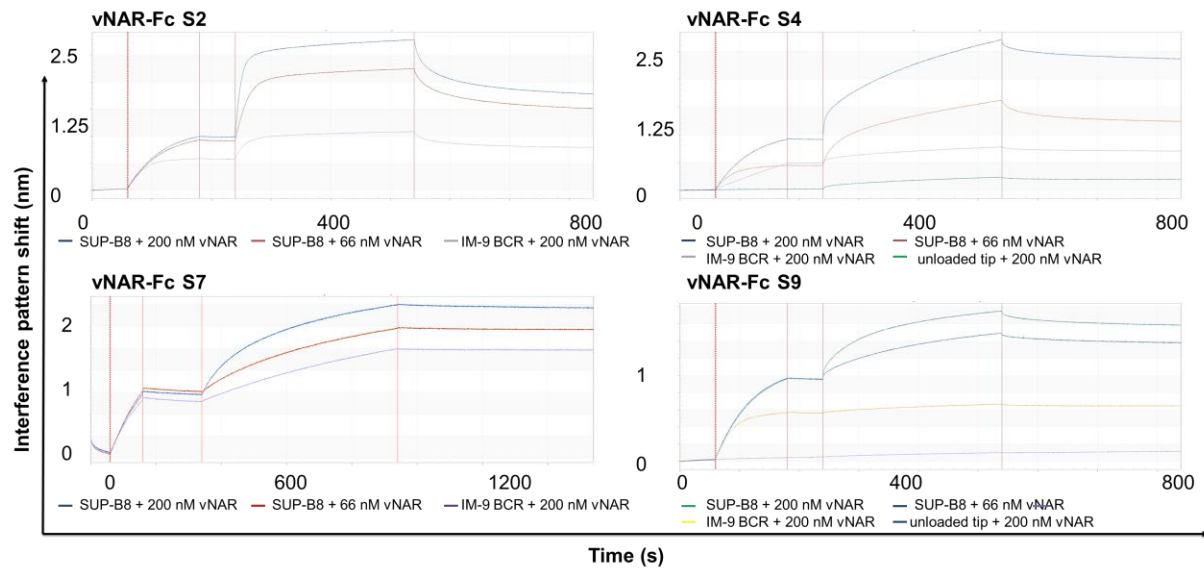
SUPPLEMENTARY FIGURE S5 | Single clone analysis after three rounds of sorting for SUP-B8 binding vNARs. Each respective single clone was measured after one day of induction. Cells were incubated with 500 nM SUP-B8 BCR, anti-human-Fc-PE conjugate served as detection antibody. For each clone a negative control in absence of antigen was performed.



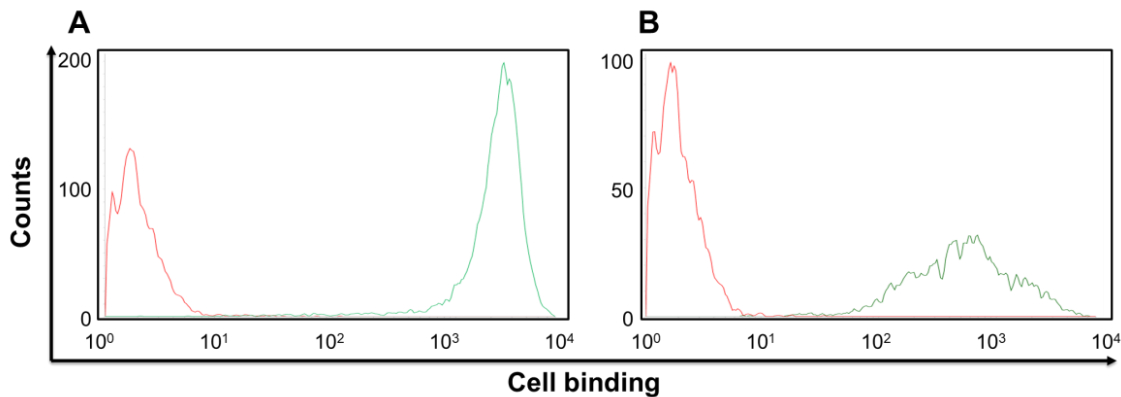
SUPPLEMENTARY FIGURE S6 | SDS-PAGE under reducing and non-reducing conditions of six vNAR-Fc constructs after Expression in HEK293 Expi cells and protein A purification. Molecular weight of vNAR-Fc molecules is approximately 80 kDa.



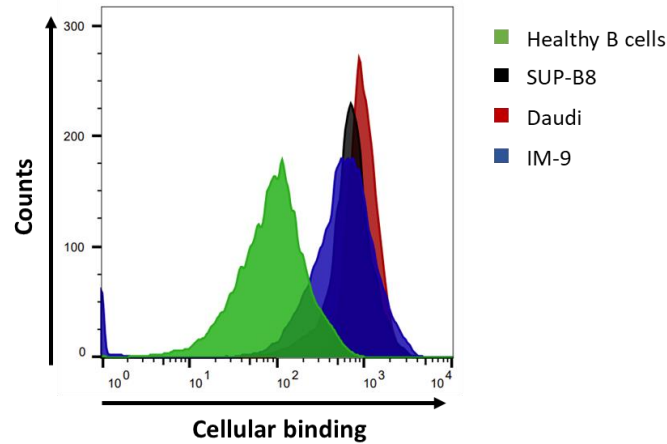
SUPPLEMENTARY FIGURE S7 | Binding kinetics of vNAR-Fc variants directed against the BCR of the SUP-B8 cell line as determined using Bio-Layer Interferometry and an Octet® RED96 system. BCR molecules were immobilized onto anti-human Fab-CH1 2nd Generation sensor tips. Association with varying concentrations of vNAR-Fc was measured for 300 or 600 s followed by dissociation measurement for 300 or 600 s. Fitting (red lines) of binding curves (colored lines) was calculated using a 1:1 binding model and Savitzky-Golay filtering. Target protein concentrations for each kinetic measurement and the resulting binding constants are depicted in each plot.



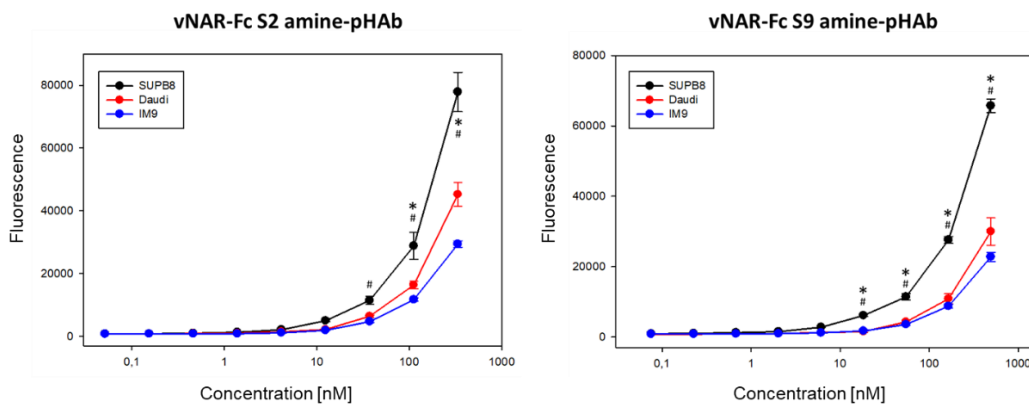
SUPPLEMENTARY FIGURE S8 | Raw Data of kinetics measurements of four vNAR-Fc variants S2, S4, S7 and S9 via biolayer interferometry with an Octet® RED96 system. BCR molecules were immobilized onto Anti-Human Fab-CH1 2nd Generation sensor tips. Association with varying concentrations of vNAR-Fc was measured for 300 or 600 s followed by dissociation measurement for 300 or 600 s. In each plot a control measurement with IM-9 BCR immobilized to the tips was implemented. Target protein concentrations for each kinetic measurement are depicted in each plot.



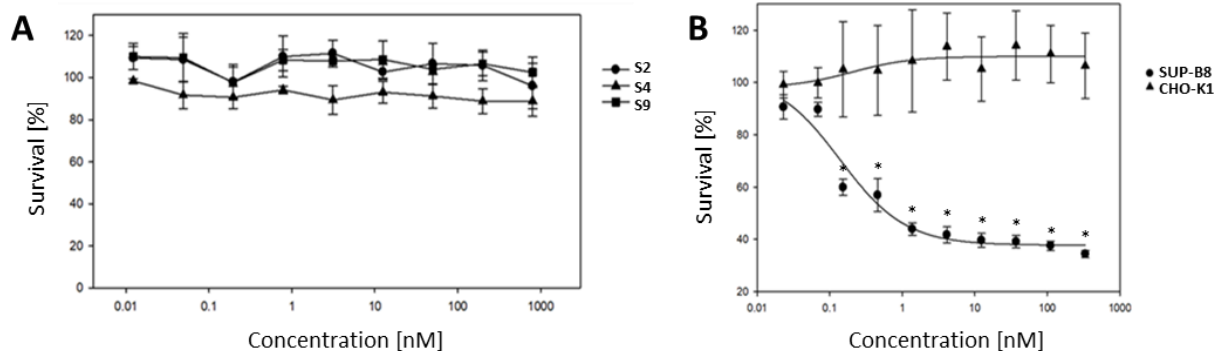
SUPPLEMENTARY FIGURE S9 | Confirmation of BCR surface expression of cell lines SUP-B8 (A) and IM-9 (B). Before measurement, cells were treated according to section 2.1. Red: unstained cells; green: anti-lambda-PE conjugate (for SUP-B8 cells) and anti-kappa-PE conjugate (for IM-9 cells). Cells were incubated 30 min on ice with the respective detection antibody.



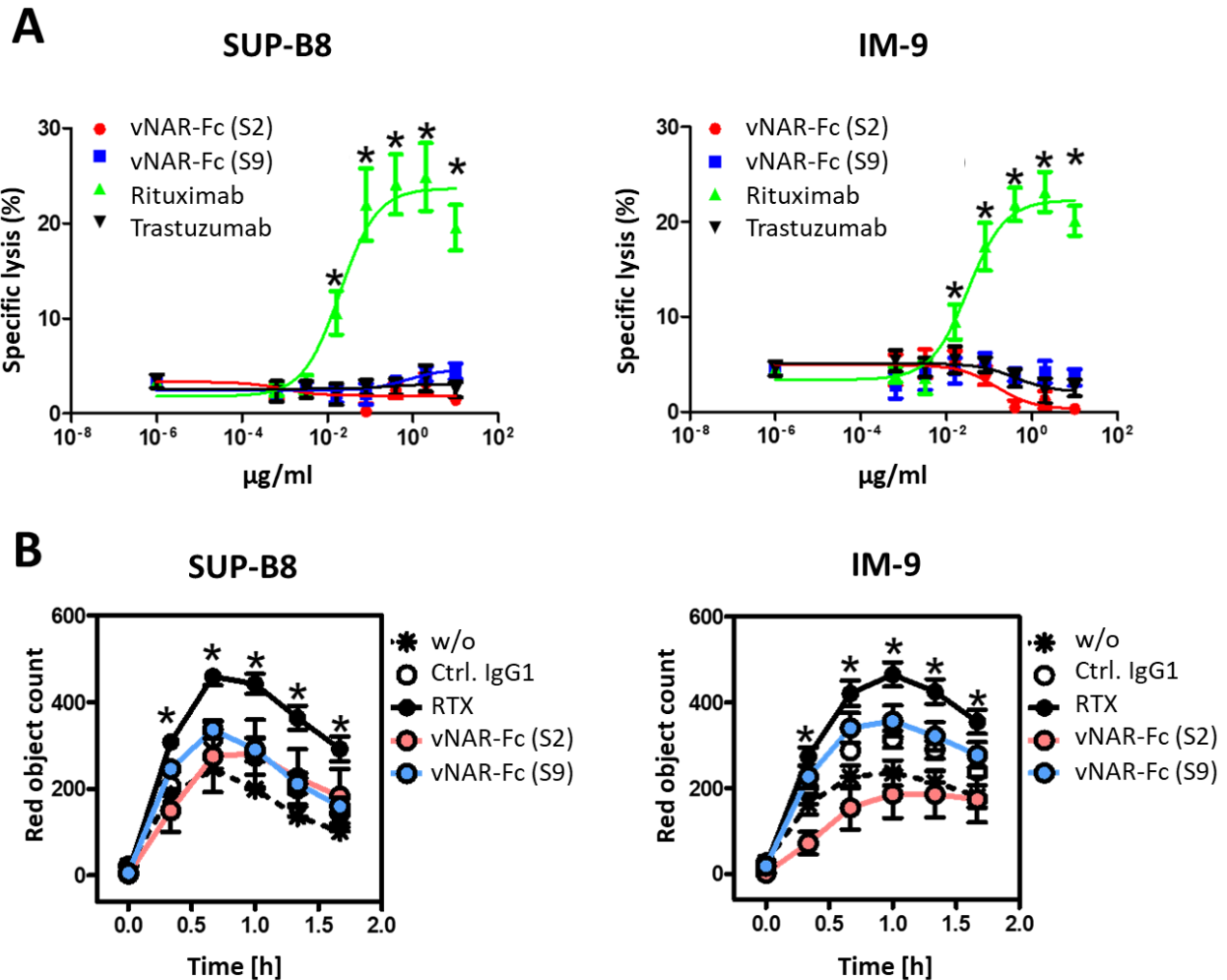
SUPPLEMENTARY FIGURE S10 | Comparison of cell surface BCR expression levels on lymphoma B cells and primary B cells isolated from healthy donors. Before analysis, cells were incubated 30 min on ice with anti-lambda-PE and anti-kappa-PE conjugates. Green: healthy B cells; black: SUP-B8; red: Daudi; blue: IM-9. Results are representative of 3 independent experiments.



SUPPLEMENTARY FIGURE S11 | Internalization assay of vNAR-Fc fusion proteins. Lymphoma B cells were treated overnight with a concentration series of amine-pHAb conjugated vNAR-Fc antibodies. Endocytosis of pHAb-conjugated antibodies can be quantified by means of increasing fluorescence at acidic pH. vNAR-Fc antibodies were conjugated with a 20 molar excess of pHAb dye and purified using a desalting column. Internalization rates were monitored at a plate reader at Ex/Em of 532 nm/560 nm. Mean \pm SEM of triplicates are plotted. Results were analyzed by two-way ANOVA (Bonferroni t-test) and significant differences ($p \leq 0.05$) between on-target SUP-B8 and control Daudi and IM-9 B cells are depicted by * and #, respectively.



SUPPLEMENTARY FIGURE S12 | Cytotoxicity assays of different vNAR-Fc variants using the MTS Cell Proliferation Assay. B-cell line SUP-B8 was treated with three bivalent vNAR-Fc variants S2, S4 and S9 at varying concentrations (12 pM – 800 nM) (A). Specificity of the vNAR-derived antibody-drug conjugates was assessed upon treatment of on-target SUP-B8 B-cells as well as unrelated CHO-K1 cells with varying concentrations of the MMAE-conjugated vNAR(S9)-Fc antibody (B). Cell proliferation assays were performed in triplicates and the relative survival after 72 h treatment was plotted against the antibody concentrations. Results are shown as mean \pm SEM and are representative of at least three independent experiments. Data were analyzed by two-way ANOVA (Bonferroni t-test), and significant differences ($p \leq 0.05$) between control and on-target cell line are depicted by *.



SUPPLEMENTARY FIGURE S13 | Fc-mediated effector functions. Mononuclear cells isolated from human blood served as effector cells in ADCC assays against lymphoma B cells. Effector cells were treated with increasing concentrations of vNAR-Fc fusion proteins and co-cultivated with SUP-B8 (on-target) or IM-9 (off-target) cells for 4 h. Rituximab and trastuzumab were used as positive and negative controls, respectively (**A**). Human macrophages served as effector cells against malignant B cells in ADCP assays. In ADCP assays, human macrophages were used as effector cells against malignant B-cells. After treatment with vNAR-Fc fusion protein, rituximab or a control IgG1 antibody, macrophages were co-cultivated for 2 h with lymphoma B cells (**B**). Results are shown as mean \pm SEM obtained from 3 independent experiments (3 effector independent donors). Data were analyzed by two-way ANOVA, and significant differences ($p \leq 0.05$) between control and specific antibodies are depicted by *.

2 Supplementary Tables

SUPPLEMENTARY TABLE S1 | Oligonucleotide primers used in this study

Name	Sequence (5' - 3')
<i>Amplification of BCR V_H and V_L</i>	
VH1-5'clon	CAGGTGCAGCTGGTGCAGTCTGG
VH2-5'clon	CAGGTCACCTTGAAGGAGTCTGG
VH3-5'clon	GAGGTGCAGCTGGTGGAGTCTGG
VH4-5'clon	CAGGTGCAGCTGCAGGAGTCGGG
VH5-5'clon	GAGGTGCAGCTGGTGCAGTCTGG
VH6-5'clon	CAGGTACAGCTGCAGCAGTCAGG
C _μ -3'	CTCTCAGGACTGATGGGAAGCC
C _μ -clon	GGAGACGAGGGGAAAAG
IgG-3'	GCCTGAGTTCACGACACC
IgG-clon	CAGGGGAAGACCGATGG
Vκ1-5'clon	GACATCCAGATGACCCAGTCTCC
Vκ2/3-5'clon	GATATTGTGATGACCCAGACTCCA
IgκC-3'	CCCCTGTTGAAGCTCTTTGT
IgκC-clon	AGATGGCGGAAGATGAAG

VL1_(51)_clon	CAGTCTGTGTTGACGCAGCCGCCCTC
VL1_(36-47)_clon	TCTGTGCTGACTCAGCCACCCTC
VL1_(40)_clon	CAGTCTGTCGTGACGCAGCCGCCCTC
VL2-clon	TCCGTGTCCGGGTCTCCTGGACAGTC
VL3-clon	ACTCAGCCACCCTCGGTGTCAGTG
VL4-clon	TCCTCTGCCTCTGCTTCCCTGGGA
VL5-clon	CAGCCTGTGCTGACTCAGCC
IGLC-3'	GTGTGGCCTTGTGGCTTG
IGLC2-7_clon	CGAGGGGGCAGCCTTGGG
IGLC1_clon	AGTGACCGTGGGGTTGGCCTTGGG
<i>Cloning for Production of B-Cell Receptors: Variable heavy chain</i>	
Daudi_HC_BamHI_up	GCTGATGTTCTGGATCCCTGCTAGCTTAAGCGAGGTGCAGCTGGTGGAGTCTGG
Daudi_HC_ApaI_lo	GGGAAGACCGATGGGCCCTTGGTGGAGGCTGAGGAGACGGTGACCAG
IM9_HC_BamHI_up	GCTGATGTTCTGGATCCCTGCTAGCTTAAGCGAGGTGCAGCTGGTGGAGTCTGGG GGAGGC
IM9_HC_ApaI_lo	GGGAAGACCGATGGGCCCTTGGTGGAGGCTGAAGAGACGATGACCAT
SUPB8_HC_BamHI_up	GCTGATGTTCTGGATCCCTGCTAGCTTAAGCCAGATTCAGCTGGTGCAGTCTGGA GGTGAG

SUPB8_HC_ApaI_lo	GGAAGACCGATGGGCCCTTGGTGGAGGCTGAGGAGACGGTGACCA
<i>Cloning for Production of B-Cell Receptors: Variable light chain</i>	
Daudi_LC_BamHI_up	GCTGATGTTCTGGATCCCTGCTAGCTTAAGCGAGCTCCAGATGACCCAGTCTCCATCCTCC
Daudi_LC_SOE_LO	GAAGACAGATGGTGCAGCCACAGTTCGTTTGTGTCCACCTT
Daudi_LC_SOE_UP	AAGGTGGACAACAAACGAACTGTGGCTGCACCATCTGTCTTC
IM9_LC_BamHI_up	GCTGATGTTCTGGATCCCTGCTAGCTTAAGCGAGCTCCAGATGACCCAGTCTCCTTCCACCCTG
IM9_LC_SOE_lo	GAAGACAGATGGTGCAGCCACAGTTCGTTTGATTTCCACCTTGGT
IM9_LC_SOE_up	ACCAAGGTGGAAATCAAACGAACTGTGGCTGCACCATCTGTCTTC
SUPB8_Lambda_NotI_lo	CCTACAGAATGTTTCGTAATAGGCGGCCG AGATCCCCGACCTC
SUPB8_LC_BamHI_up	GCTGATGTTCTGGATCCCTGCTAGCTTAAGCCAGTCTGTGTTGACGCAGCCG
SUPB8_LC_SOE_lo	TGGCGGGAACAGAGTGACCGAGGGGGCAGCCTTGGG
SUPB8_LC_SOE_up	CCCAAGGCTGCCCCCTCGGTCACTCTGTTCCCGCCA
SUPB8_Lambda_NotI_lo	GAGGTGGGGGATCTGCGGCCGCTATTACGAACATTCTGTAGG
<i>Sequencing</i>	
pCT_seq_up	TACCCATACGACGTTCCAGACTAC
pCT_seq_lo	CAGTGGGAACAAAGTCGATTTTGTAC

pExp_seq_up	GAGAACCCACTGCTTACTGGC
pExp_seq_lo	CACGCCGTCCACATACCAGTTGAAC
<i>Expression</i>	
pExp_NheI_up	GCGCGCGCTAGCCGCTGAGAACCTGTA CTTCAGAGCGCCGTGACGTTGGACGAG
pExp_F1_lo	GGTGTGGGTCTTGTCGCAGCTCTTGGGCTCGCTTCCGCTCTGGAAGTACAGGTTCT CTTTCACAGTCAGAGTGGTGCCGCCTCC
pExp_F2_lo	GGTGTGGGTCTTGTCGCAGCTCTTGGGCTCGCTTCCGCTCTGGAAGTACAGGTTCT CTTTCACAGTCAGAGTGGTGCCGCCCCCTTC
pExp_F4_lo	GGTGTGGGTCTTGTCGCAGCTCTTGGGCTCGCTTCCGCTCTGGAAGTACAGGTTCT CTTTCACAGTCAGAATGGTCCCCCTCC
pExp_F7_lo	GGTGTGGGTCTTGTCGCAGCTCTTGGGCTCGCTTCCGCTCTGGAAGTACAGGTTCT CTTTCACAGTCACAGTGGTGCCCCCACC
pExp_F8_lo	GGTGTGGGTCTTGTCGCAGCTCTTGGGCTCGCTTCCGCTCTGGAAGTACAGGTTCT CTTTCACAGTCAGAGTGGTCCCGCCGCC
pExp_L1_lo	GGTGTGGGTCTTGTCGCAGCTCTTGGGCTCGCTTCCGCTCTGGAAGTACAGGTTCT CTTTCACAGTCACAGTGGTCCCCCTCC
pExp_L3_lo	GGTGTGGGTCTTGTCGCAGCTCTTGGGCTCGCTTCCGCTCTGGAAGTACAGGTTCT CTTTCACAGTCACAGTGGTGCCGCCACC
pExp_ApaI_lo	GCGCGCGGGCCCCGCCAGCAGTTCAGGGGCAGGGCAGGGAGGACAGGTGTGGGTC TTGTCGCAGCTCTTGGGCTCGCTTCC